

Thermodynamically stable single-side hydrogenated graphene

H. J. Xiang,¹ E. J. Kan,² Su-Huai Wei,³ X. G. Gong,¹ and M.-H. Whangbo²

¹Key Laboratory of Computational Physical Sciences, Ministry of Education, and Department of Physics, Fudan University, Shanghai 200433, People's Republic of China

²Department of Chemistry, North Carolina State University, Raleigh, North Carolina 27695-8204, USA

³National Renewable Energy Laboratory, Golden, Colorado 80401, USA

(Received 29 August 2010; published 13 October 2010)

The single-sided hydrogenation of graphene was examined by combining the cluster expansion method with density-functional theory to find that hydrogen atoms prefer to form one-dimensional chains, leading to ripples made up of sp^2 carbon atoms between them. The formation of such novel structures is due to the competition between electronic kinetic energy and elastic strain energy. Surprisingly, the single-sided hydrogenation of graphene is thermodynamically stable at low hydrogen coverage, and some hydrogenated graphenes are semiconducting, similar to graphene nanoribbons. The new single-side hydrogenated graphene structures account for several puzzling experimental observations. In addition, we propose a low-energy single-side fluorinated graphene structure.

DOI: [10.1103/PhysRevB.82.165425](https://doi.org/10.1103/PhysRevB.82.165425)

PACS number(s): 61.48.Gh, 71.20.-b, 73.22.-f, 73.61.Wp

I. INTRODUCTION

Graphene, a single layer of carbon atoms arranged in a honeycomb lattice, has been the focus of recent research efforts,¹⁻³ due to its unique zero-gap electronic structure and the massless Dirac fermion behavior. The unusual electronic and structural properties make graphene a promising material for the next generation of faster and smaller electronic devices. Chemical functionalization is a way to modify the electronic and crystal structure of graphene, which may be important for graphene-based nanoelectronics.⁴⁻⁹ The hydrogenation of graphene,^{4,5,7} as a prototype of covalent chemical functionalization, is of fundamental importance. The double-sided hydrogenation of graphene is now well understood, at least from the theoretical point of view. For example, Sofo *et al.*¹⁰ predicted theoretically a new insulating material called graphane, in which each hydrogen atom adsorbs on top of a carbon atom from both sides. The formation of graphane was attributed to the efficient strain relaxation for the sp^3 hybridization.¹¹

The prediction for the hydrogenated graphene was partially confirmed by Elias *et al.*¹² who demonstrated that graphene can react with atomic hydrogen, which transforms this highly conductive zero-overlap semimetal into an insulator, and hydrogenation of graphene is reversible. However, in the case of graphene on a substrate such as SiO_2 ,¹² hydrogenation can occur only on the top basal plane of graphene because the diffusion of hydrogen along the graphene- SiO_2 interface is negligible and perfect graphene is impermeable to any atom and molecule.¹³ Previous theoretical studies^{14,15} suggest that single-sided hydrogenation of ideal graphene would be thermodynamically unstable. Thus, it remains a puzzle why the hydrogenation of graphene on a substrate is possible and the hydrogenated species are stable at room temperature.^{12,16}

To address the aforementioned issues, we examine the single-sided hydrogenation of graphene by combining the cluster-expansion method¹⁷ with density functional theory. We find that hydrogen atoms tend to form one-dimensional

(1D) chains leading to ripples made up of sp^2 carbon atoms between them. Surprisingly, the single-sided hydrogenation of graphene is thermodynamically stable at low hydrogen coverage, and some of the new single side hydrogenated graphene are semiconducting, similar to graphene nanoribbons (GNRs). In contrast to the case of the double-sided hydrogenation, the phase separation is unstable in single-side hydrogenated graphene, which suggests that the single-sided functionalization might be a better way of tuning the electronic properties of graphene.

II. COMPUTATIONAL METHOD

It is well known that a hydrogen atom adsorbs on the top of a carbon atom in graphenelike systems. We treat the single-side hydrogenated graphene as an alloy system in which a vacancy or a hydrogen atom could occupy the top sites above the graphene basal plane, as shown in Fig. 1(a). To find the lowest energy structure of graphene with different coverages of hydrogen atoms, we use the state of the art

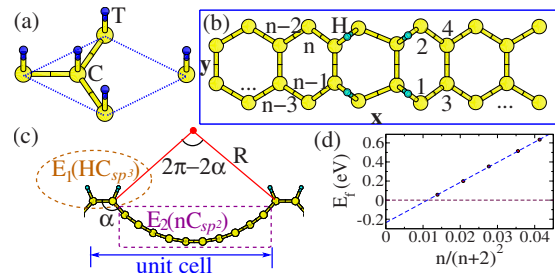


FIG. 1. (Color online) (a) The CT structure used in the cluster expansion calculations. “T” refers to the top site above the basal plane of graphene. (b) The top view of a 2H-AG structure. The unit cell is enclosed by a rectangle. The numbers denote the sp^2 carbon atoms. (c) The decomposition of 2H-AG into two parts: the sp^3 hybridized C-H part and sp^2 carbon part. (d) The formation energy of 2H-AG as a function of $n/(n+2)^2$ (n is the number of sp^2 carbon atoms). The line is fitted according to Eq. (3).

“cluster-expansion” method¹⁷ established in the alloy theory in which the alloy Hamiltonian is mapped onto a generalized Ising Hamiltonian. In brief, for some adsorption configurations, we perform spin-polarized DFT calculations to relax the cell and internal atomic coordinates. The energies of the relaxed structures are used to extract the interaction parameters of the alloy Hamiltonian. The mapping process was carried out by the ATAT package.¹⁸

In our DFT calculations, the local density approximation (LDA) was adopted and the plane-wave cut-off energy for wave function was set to 500 eV. The ion-electron interaction was treated using the projector augmented wave¹⁹ technique as implemented in the Vienna *ab initio* simulation package.²⁰

III. RESULTS AND DISCUSSION

After obtaining the interaction parameters (nine pair interaction parameters and four three-body interaction parameters) of the alloy Hamiltonian, we can predict the energy of single-side hydrogenated graphene with any adsorption pattern. To identify the most favorable hydrogen adsorption configuration, we define the average adsorption energy at concentration y/x as

$$E_a = [E(C_xH_y) - x\mu_C - y\mu_H]/y, \quad (1)$$

where $E(C_xH_y)$ is the total energy of the hydrogenated graphene, and μ_C and μ_H are set to those of graphene and hydrogen molecule, respectively. It is noted that the difference in E_a between two adsorption configurations does not depend on μ_H . If E_a is negative, the adsorption process is exothermic and the hydrogenated graphene is thermodynamically stable. E_a for the double-side hydrogenated graphene, i.e., graphane, is as low as -0.397 eV/H, in accord with its high stability. We generate all nonequivalent adsorption configurations for all unique supercells with less than 24 carbon atoms using the linear scaling algorithm recently proposed by Hart and Forcade.²¹ Our calculations using the alloy Hamiltonian show that the adsorption configurations with the lowest average adsorption energies have the adsorption pattern shown in Fig. 1(b). In this structure, the hydrogen atoms form 1D armchair chains. The width of the armchair chain is two according to the conventional definition¹¹ of armchair GNRs (AGNR). Hereafter this kind of adsorption configuration is referred to 2H-AG. As can be seen from Fig. 1(c), the sp^2 carbon atoms form an arch since the angles between a sp^3 carbon atom and its neighbors tend to be 109.47° . The average adsorption energy is found to be 0.12 eV/H, indicating that the adsorption configuration is thermodynamically unstable at this hydrogen coverage (i.e., $H_c=1/6$).

The hydrogenated graphene shown in Figs. 1(b) and 1(c) consists of two parts: the sp^3 hybridized C-H part and sp^2 carbon part. Thus, we can decompose its formation energy (per unit cell) with respect to graphene and H_2 into two components

$$E_f = E_1(HC_{sp^3}) + E_2(nC_{sp^2}), \quad (2)$$

where n represents the number of sp^2 carbon atoms [see Fig. 1(b)]. The formation energy of the sp^2 carbon part $E_2(nC_{sp^2})$

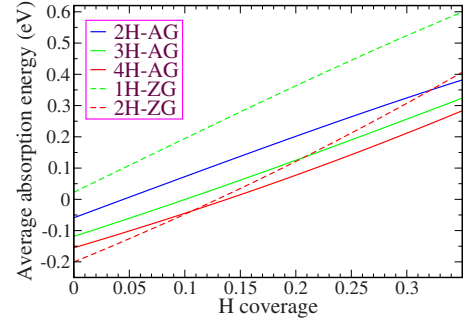


FIG. 2. (Color online) The average adsorption energies as a function of H coverage for 2H-AG, 3H-AG, 4H-AG, 1H-ZG, and 2H-ZG. The average adsorption energies are calculated using the formation energy according to Eq. (3) with the parameters fitted from DFT energies. The zero average adsorption is indicated by the horizontal line.

is due to the elastic strain: $E_2(nC_{sp^2})=E_s$. The bent sp^2 carbon part can be seen as a part of a carbon nanotube. For carbon nanotubes, the strain energy per carbon atom is inversely proportional to the square of the radius (R) of the tube.²² Thus, $E_s=nA/R^2$ (A is a constant), and R can be calculated as $(\frac{n}{2}+1)\frac{\sqrt{3}}{2}b_{CC}/(2\pi-2\alpha)$ [b_{CC} is the sp^2 C-C bond length (1.42 Å), and α is the bending angle as a result of the hydrogen adsorption, see Fig. 1(c)]. The reason for the energy decomposition is that the elastic strain energy is not fully described by the short range cluster-expansion Hamiltonian. Finally, we obtain

$$E_f = E_1(HC_{sp^3}) + nB/(n+2)^2 \quad (3)$$

with $B = \frac{64A(\pi-\alpha)^2}{3b_{CC}^2}$. This means that when n goes to infinity, the total strain energy becomes zero, and the formation energy is solely determined by $E_1(HC_{sp^3})$. We construct several other adsorption configurations similar to that shown in Fig. 1(b) but with different number of sp^2 carbon atoms. The formation energies as a function of n are fitted according to Eq. (3) via parameters $E_1(HC_{sp^3})$ and B . The good linear correlation between E_f and $n/(n+2)^2$ can be clearly seen from Fig. 1(d). The least-squares fitting gives $E_1(HC_{sp^3}) = -0.236$ eV and $B = 21.112$ eV. The negative value of $E_1(HC_{sp^3})$ suggests that the adsorption pattern shown in Fig. 1(c) becomes thermodynamically stable when $n \geq 86$.

A previous study suggested that in double-side hydrogenated graphene, the hydrogen atoms tend to adsorb on neighboring carbon atoms in order to maximize the number of sp^2 C-C bonds.¹¹ To see whether the clustering of hydrogen armchair lines leads to a lower average adsorption energy, we double the cell of Fig. 1(b) along the x direction and move the hydrogen armchair lines next to each other. As expected, the bending angle α in the optimized structure is much smaller than that of the 2H-AG case. The calculated DFT average adsorption energy for the 4H-AG is 0.039 eV/H, which is indeed lower compared with the case presented in Fig. 1(b). This result prompted us to find out the dependence of the formation energy upon the number of sp^2 carbon atoms for the 3H-AG and 4H-AG cases. Figure 2 plots the average adsorption energy as a function of hydrogen cover-

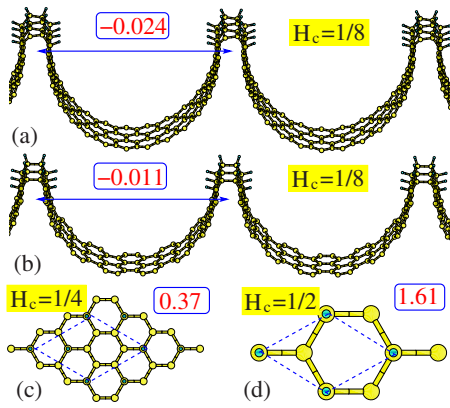


FIG. 3. (Color online) Structures of (a) 4H-AG with $n=56$, (b) 2H-ZG with $n=28$, (c) single-side hydrogenated graphene proposed in Ref. 6, and (d) single-side hydrogenated graphene proposed in Ref. 15. The numbers (in eV/H) in rectangles denote the average adsorption energies. The unit cells are marked. The hydrogen coverages (H_c) are shown.

age. We can see that the 4H-AG has a lowest E_a for a given H coverage and E_a decreases with increasing the number of H armchair lines. This is consistent with the fact that the clustering of hydrogen armchair lines leads to a lowering of the kinetic energy of sp^2 carbon π electrons. However, it should be noted that the adsorption configuration with the number of H armchair lines larger than four has a higher energy because the bending angle is much smaller than 90° and the associated steric repulsion is too large. A 4H-AG structure (0.125 H coverage) with a negative E_a is shown in Fig. 3(a). It is seen that the number of sp^2 carbon atoms is the same between every two hydrogen lines as a consequence of the periodic boundary condition. As a matter of fact, this uniformly spaced structure has a lower energy than other structures because the strain energy is minimized when $m=0$ [$2n/(n+2)^2 < (n-m)/(n-m+2)^2 + (n+m)/(n+m+2)^2$, when $m > 0$ and $n \geq 2$]. The average adsorption energy increases with hydrogen coverage due to the increased strain energy. When the H coverage H_c is less than 0.138, single-sided hydrogen adsorption is thermodynamically stable.

We now consider the possibility of the formation of zigzag H chains. In this case, no more than two zigzag H chains can exist due to the steric repulsion. The formation energy can be expressed as: $E_f = E_1(HC_{sp^3} + nB/(n+4/3)^2)$, which is slightly different from Eq. (3) due to the difference in geometry. As shown in Fig. 2, the 1H-zigzag graphene (1H-ZG) has a high average adsorption energy and is thermodynamically unstable for any H coverage. Interestingly, the 2H-zigzag graphene (2H-ZG) has the lowest average adsorption energy in the limit of zero H coverage among all adsorption configurations. However, the average adsorption energy increases faster with H coverage than that in the 4H-zigzag graphene (4H-AG) case because α in 2H-ZG is smaller. As a result, there is a crossover point at $H_c=0.107$ below (above) which the 2H-ZG (4H-AG) is the most stable adsorption configuration. A 2H-ZG structure with 0.125 H coverage is shown in Fig. 3(b). The average hydrogen adsorption energy E_a is negative (i.e., -0.011 eV/H) but larger than that for the 4H-AG with the same H coverage shown in Fig. 3(a).

This is in agreement with the trend shown in Fig. 2.

The thermodynamically stable single-side hydrogenated graphene structures from our study are nontrivial and unexpected. The peculiar adsorption configuration is a consequence of the competition between electronic kinetic energy and elastic strain energy: the hydrogen atoms tend to be close to each other to lower the kinetic energy of carbon π electrons while the full phase separation between sp^3 carbon part and sp^2 graphene is prohibited by the large strain caused by the single-sided hydrogen adsorption. Previous studies suggested two possible single-side hydrogenated graphene structures. One structure [Fig. 3(c)] was constructed based on the observation that the optimal way for the one-side chemisorption of two hydrogen atoms on graphene is to occupy the (1,4) positions.¹⁴ This 0.25 H coverage structure has an average hydrogen adsorption of 0.37 eV/H, which is higher than that (about 0.137 eV/H) for the 4H-AG case (see Fig. 2). This suggests that the macroscopic single-sided hydrogen adsorption on graphene is a cooperative phenomenon, which can hardly be described by the adsorption preference of a small number of hydrogen atoms. Another proposed single-side hydrogenated graphene structure [Fig. 3(d)] can be constructed by removing all the bottom hydrogen atoms from graphene and was suggested to be ferromagnetic.¹⁵ This 0.5 H coverage has a very high E_a of 1.61 eV/H, which is much higher than that (about 0.465 eV/H) of the corresponding 4H-AG structure. It should be noted that even with the same H coverage (0.25 or 0.5), the single-side hydrogenated graphene structure based on our new bent models has a much lower energy although the single-side hydrogenated graphene is thermodynamically unstable at this H coverage.

The new bent single-side hydrogenated graphene structures might account for some experimental observations. The formation of bent single-side hydrogenated graphene structures is thermodynamically possible with a negative but small adsorption energy. This is in accord with the fact that hydrogenated graphene is stable at room temperature but the original metallic state can be restored by annealing at 450°C in Ar atmosphere for 24 h.¹²

Very recently, graphene films grown on Cu foils have been fluorinated with xenon difluoride (XeF_2) gas.²³ It was found that for single-side fluorinated graphene, the F coverage saturates at 25% (C_4F). Through DFT calculations, Robinson *et al.*²³ proposed a C_4F structure which can be obtained by replacing H by F in the structure shown in Fig. 3(c). It was suggested that the C_4F structure similar to that shown in Fig. 3(c) has the largest binding energy per F atom. Our calculations show that the 2F-ZG structure with $n=12$ (similar to the structure shown in Fig. 3(b) but with a 25% F coverage) has a lower energy than the previously proposed C_4F structure by about 0.15 eV/F. This result suggests that the bent single-side hydrogenated graphene structures might be also relevant to the single-side functionalization of graphene by other atoms or groups.

Finally, we discuss the electronic properties of new single-side hydrogenated graphene structures, i.e., 4H-AG and 2H-ZG. The band structure for 4H-AG with $n=56$ [Fig. 3(a)] is shown in Fig. 4(a). For comparison, the band structure of 28-AGNR which has the same number of sp^2 carbon atoms as the 4H-AG is also plotted. The 4H-AG has a similar

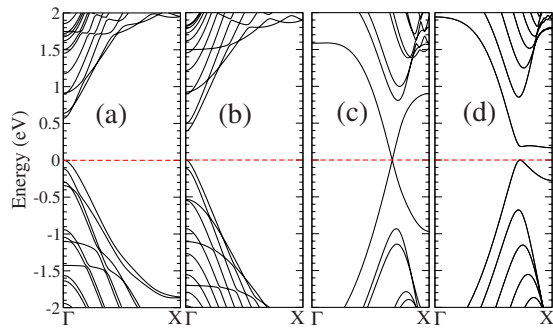


FIG. 4. (Color online) LDA band structures of (a) 4H-AG with $n=56$, (b) 28-AGNR, (c) 2H-ZG with $n=28$, and (d) 14-ZGNR with the antiferromagnetic state.

band structure as does 28-AGNR except that the 4H-AG has a slightly larger band gap possibly due to the curvature effect. Figures 4(c) and 4(d) show the band structures of the 2H-ZG with $n=28$ [Fig. 3(b)] and 14-Zigzag GNR (ZGNR), respectively. It is well-known that a ZGNR has local moments at two edges and an antiferromagnetic alignment between two edges results in a small band-gap opening [Fig. 4(d)]. In the case of 2H-ZG, there is no local spin moments. This is because the degenerate edge states can interact with each other resulting in energy lowering by occupying the bonding state. The band gap is closed at the Dirac point $\mathbf{k} \approx (0.34, 0, 0)$.

IV. CONCLUSION

In summary, we studied the single-side hydrogenation of graphene by combining the cluster-expansion method with density-functional theory, to find that hydrogen atoms tend to form 1D chains with ripples made up of sp^2 carbon atoms between them. We reveal that the single-sided hydrogenation of graphene is thermodynamically stable at low hydrogen coverage. The small magnitude of the adsorption energy is in accord with the reversible hydrogenation observed experimentally. In contrast to the case of double-sided hydrogenation, the phase separation in single-side hydrogenated graphene is unstable, hence suggesting that single-sided covalent functionalization might be a better way to tune the electronic properties of graphene. In addition, we find a different single-side fluorinated graphene structure which has a lower energy than the previously proposed model.

ACKNOWLEDGMENTS

Work at Fudan was partially supported by the National Science Foundation of China, Pujiang plan, and the Program for Professor of Special Appointment (Eastern Scholar) at Shanghai Institutions of Higher Learning. Work at NREL was supported by the U.S. Department of Energy under Contract No. DE-AC36-08GO28308. M.H.W. thanks the financial support from U.S. DOE under Grant No. DE-FG02-86ER45259.

- ¹K. S. Novoselov, A. K. Geim, S. V. Morozov, D. Jiang, M. I. Katsnelson, I. V. Grigorieva, S. V. Dubonos, and A. A. Firsov, *Nature (London)* **438**, 197 (2005).
- ²K. S. Novoselov, E. McCann, S. V. Morozov, V. I. Falko, M. I. Katsnelson, U. Zeitler, D. Jiang, F. Schedin, and A. K. Geim, *Nat. Phys.* **2**, 177 (2006).
- ³Y. B. Zhang, Y. W. Tan, H. L. Stormer, and P. Kim, *Nature (London)* **438**, 201 (2005).
- ⁴E. Bekyarova, M. E. Itkis, P. Ramesh, C. Berger, M. Sprinkle, W. A. de Heer, and R. C. Haddon, *J. Am. Chem. Soc.* **131**, 1336 (2009).
- ⁵S. Ryu, M. Y. Han, J. Maultzsch, T. F. Heinz, P. Kim, M. L. Steigerwald, and L. E. Brus, *Nano Lett.* **8**, 4597 (2008).
- ⁶D. W. Boukhvalov and M. I. Katsnelson, *Nano Lett.* **8**, 4373 (2008).
- ⁷D. W. Boukhvalov and M. I. Katsnelson, *J. Phys.: Condens. Matter* **21**, 344205 (2009).
- ⁸N. Lu, Z. Li, and J. Yang, *J. Phys. Chem. C* **113**, 16741 (2009).
- ⁹H. J. Xiang, S.-H. Wei, and X. G. Gong, *Phys. Rev. B* **82**, 035416 (2010).
- ¹⁰J. O. Sofo, A. S. Chaudhari, and G. D. Barber, *Phys. Rev. B* **75**, 153401 (2007).
- ¹¹H. J. Xiang, E. J. Kan, S.-H. Wei, M.-H. Whangbo, and J. L. Yang, *Nano Lett.* **9**, 4025 (2009).
- ¹²D. C. Elias, R. R. Nair, T. M. G. Mohiuddin, S. V. Morozov, P. Blake, M. P. Halsall, A. C. Ferrari, D. W. Boukhvalov, M. I. Katsnelson, A. K. Geim, and K. S. Novoselov, *Science* **323**, 610 (2009).
- ¹³D. Jiang, V. R. Cooper, and S. Dai, *Nano Lett.* **9**, 4019 (2009). Our test calculations show that the barrier for the penetration of a hydrogen atom through the six-membered ring of graphene is larger than 2.0 eV.
- ¹⁴D. W. Boukhvalov and M. I. Katsnelson, *Phys. Rev. B* **78**, 085413 (2008).
- ¹⁵J. Zhou, Q. Wang, Q. Sun, X. S. Chen, Y. Kawazoe, and P. Jena, *Nano Lett.* **9**, 3867 (2009).
- ¹⁶P. Sessi, J. R. Guest, M. Bode, and N. P. Guisinger, *Nano Lett.* **9**, 4343 (2009).
- ¹⁷L. G. Ferreira, S.-H. Wei, and A. Zunger, *Phys. Rev. B* **40**, 3197 (1989).
- ¹⁸A. van de Walle, M. Asta, and G. Ceder, *CALPHAD: Comput. Coupling Phase Diagrams Thermochem.* **26**, 539 (2002).
- ¹⁹P. E. Blöchl, *Phys. Rev. B* **50**, 17953 (1994); G. Kresse and D. Joubert, *ibid.* **59**, 1758 (1999).
- ²⁰G. Kresse and J. Furthmüller, *Comput. Mater. Sci.* **6**, 15 (1996); *Phys. Rev. B* **54**, 11169 (1996).
- ²¹G. L. W. Hart and R. W. Forcade, *Phys. Rev. B* **80**, 014120 (2009).
- ²²K. N. Kudin, G. E. Scuseria, and B. I. Yakobson, *Phys. Rev. B* **64**, 235406 (2001).
- ²³J. T. Robinson, J. S. Burgess, C. E. Junkermeier, S. C. Badescu, T. L. Reinecke, F. K. Perkins, M. K. Zalalutdniov, J. W. Baldwin, J. C. Culbertson, P. E. Sheehan, and E. S. Snow, *Nano Lett.* **10**, 3001 (2010).